

Article

# Hybrid Off-Grid SPV/WTG Power System for Remote Cellular Base Stations Towards Green and Sustainable Cellular Networks in South Korea

Mohammed H. Alsharif \* and Jeong Kim

Department of Electrical Engineering, College of Electronics and Information Engineering, Sejong University, 209 Neungdong-ro, Gwangjin-gu, Seoul 05006, Korea; kimjeong@sejong.ac.kr

\* Correspondence: malsharif@sejong.ac.kr; Tel.: +82-2-6935-2439; Fax: +82-2-3408-4329

Academic Editor: Adrian Ilinca

Received: 21 August 2016; Accepted: 16 December 2016; Published: 23 December 2016

**Abstract:** This paper aims to address the sustainability of power resources and environmental conditions for telecommunication base stations (BSs) at off-grid sites. Accordingly, this study examined the feasibility of using a hybrid solar photovoltaic (SPV)/wind turbine generator (WTG) system to feed the remote Long Term Evolution-macro base stations at off-grid sites of South Korea the energy necessary to minimise both the operational expenditure and greenhouse gas emissions. Three key aspects have been discussed: (i) optimal system architecture; (ii) energy yield analysis; and (iii) economic analysis. In addition, this study compares the feasibility of using a hybrid SPV/WTG system vs. a diesel generator. The simulation results show that by applying the proposed SPV/WTG system scheme to the cellular system, the total operational expenditure can be up to 48.52% more efficient and sustainability can be ensured with better planning by providing cleaner energy.

**Keywords:** hybrid energy system; remote sites; cellular networks; operational expenditure; South Korea

## 1. Introduction

Mobile communication is one of the most successful technological innovations in modern history. However, the Long Term Evolution (LTE, also known as pre-4G, i.e., 3.9G) of a cellular network is considered to be the fastest developing technology in mobile communication [1]. In addition, South Korea has witnessed tremendous development in the LTE cellular network in the last five years [2]. Today, South Korea has an LTE cellular network unrivalled in both technology and reliability, with the best global coverage (97% of the time on LTE) [3]. The LTE network offers data-oriented services that include, but are not limited to, multimedia communications, online gaming, and high-quality video streaming. As a result, the number of mobile subscribers has increased exponentially, prompting the mobile operators to significantly increase the number of LTE BSs to meet the needs of mobile subscribers. In 2013, the number of LTE BSs was 35,255 units; that number increased by 4.7-fold in 2015 to 165,193 LTE BSs [2]. This increase of LTE BSs led to increases in both the energy consumption and operational expenditure (OPEX) as a result of the LTE BS being the primary source of energy consumption in cellular networks, accounting for 57% of the total energy used [4,5]. Moreover, cellular network operators are continually seeking to increase their network coverage areas, provide services to potential customers in rural areas, and open new markets to increase profitability. Diesel generators (DGs) are typically used for power at off-grid BS sites because extending the grid connection to power off-grid BS sites is not economically attractive or existing grid electricity is not available because of geographical limitations [6]. Today, the idea of using diesel generators as a primary power supply has become less favourable because of the challenges linked to their reliability, availability, high operational and maintenance (O&M) costs, and significant environmental impacts [7].

It is now acknowledged that the LTE cellular communication network in South Korea will have greater economic and ecological impact in the coming years. The key features for power sources, such as economic, environmental, and social sustainability, of BS sites are a critically important issue. Power shortages are not allowed in the cellular mobile sector or during service outages. The specific power supply requirements for off-grid BSs, such as cost-effectiveness, efficiency, sustainability and reliability, can be met by utilising the technological advances in renewable energy [6]. The Korean government continually seeks to increase energy independence by expanding renewable energy to enable more efficient development and ensure sustainability with better planning to provide cleaner energy [8].

This study aims to give a holistic view of the sustainable power supply solution for an off-grid LTE-macro BS based on the characteristics of South Korea average solar radiation exposure and wind speed. The key contributions in this paper are summarised as follows:

1. To determine the optimal size and technical criteria of the hybrid SPV/WTG system to feed LTE-macro BS deployment at off-grid sites of South Korea. The optimum criteria, including economic, technical, and environmental feasibility parameters, were analysed by the *Hybrid Optimisation Model for Electric Renewable* (HOMER).
2. To analyse and evaluate the feasibility of using a hybrid SPV/WTG system in terms of the energy yield and economic feasibility over the project lifetime.
3. To analyse and compare the implications of choosing a hybrid SPV/WTG system with respect to a classical DG powered solution in terms of the (i) OPEX savings to maintain profitability for cellular network operators and (ii) GHG emissions that have a bad effect on the environment.

The rest of this paper is organised as follows: Section 2 presents the related work. In Section 3, the system architecture for the hybrid SPV/WTG system to supply LTE-macro BS is described, and Section 4 presents the mathematical model. Section 5 includes the system implementation and configuration, and Section 6 presents the optimization results and discussion. Section 7 presents the comparison and estimation of the feasibility of using the SPV/WTG system approach with the classical solution DG, and Section 8 concludes this paper.

## 2. Power Supply and Energy Storage Solutions for Off-Grid Base Stations

Following the emerging concept of green telecommunication networks, the realization of powering BS sites using sustainable solutions has started to receive significant attention. Therefore, various studies and developments have been done to help telecom operators shift away from using diesel generators as their primary power supply solution for BSs. It is being realized that by moving away from diesel generators, the unreliability factors and the high O&M costs usually associated with this solution can be avoided. This section summarises the renewable energy solutions in the telecommunication sector and highlights the various power supply and energy storage solutions for off-grid BSs that have been proposed. Figure 1 provides a summary of related works that have investigated green wireless network optimisation strategies within smart grid environments. In addition, Derrick et al. [9] have studied resource allocation algorithm design for energy-efficient communication in an orthogonal frequency-division multiple access (OFDMA) downlink network with hybrid energy harvesting BS. Reference [10] has discussed a point-to-point communication link where the transmitter has a hybrid supply of energy. Specifically, the hybrid energy is supplied by a constant energy source and an energy harvester, which harvests energy from its surrounding environment and stores it in a battery which suffers from energy leakage.



**Figure 1.** Summary of related works of green wireless network optimisation strategies within smart grid environments [11–19].

In addition, in a study conducted by the GSMA, which is a mobile trade organization, 320,100 renewable-based off-grid BS sites have already been rolled out in 2014. This number is expected to increase further in 2020 with about 389,800 sites [20].

### 3. System Architecture

Figure 2 is a schematic showing two subsystems: the LTE-macro BS and the hybrid SPV/WTG power subsystem.

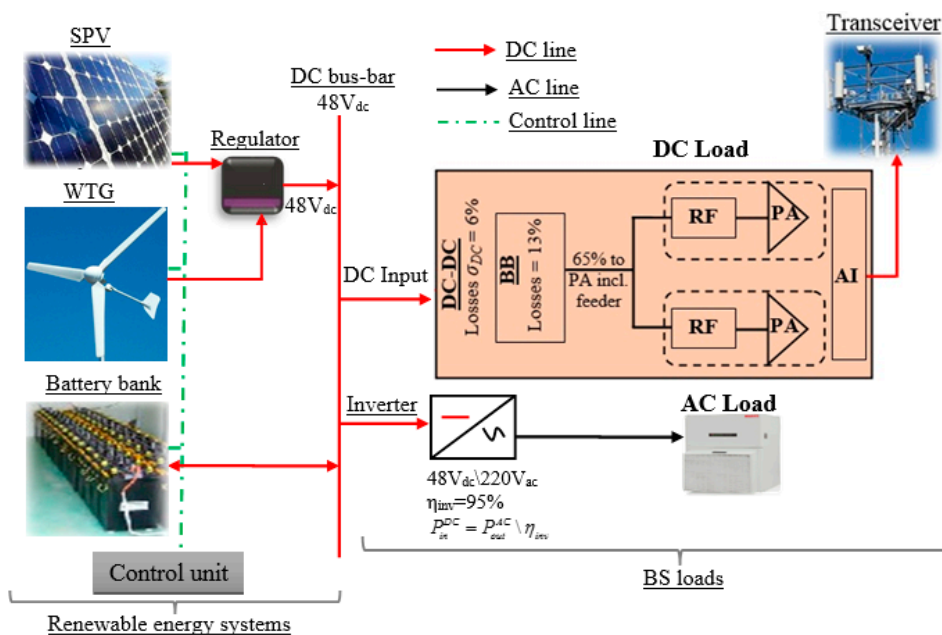


**Figure 2.** System model of the hybrid SPV/WTG power scheme for an LTE-macro BS.

### 3.1. LTE Macro-BS Subsystem and Power Consumption Modeling

The BS, a centrally located set of equipment used to communicate with mobile units and the backhaul network, consists of multiple transceivers that in turn consist of a power amplifier that amplifies the input power, a radio-frequency small-signal transceiver section, a baseband for system processing and coding, a DC-DC power supply, and a cooling system. More details on the BS components can be found in [21].

An LTE-macro BS type is described in [22] with a focus on the component level for three sectors; each BS contains two antennas. BS operating power is expressed as  $P_{op} = N_{TRX} \times (P_{PA}^{DC} + P_{RF}^{DC} + P_{BB}^{DC}) / (1 - \sigma_{DC})(1 - \sigma_{cool})$ , where  $N_{TRX}$  is the number of transceivers (i.e., transmit/receive antennas per site);  $P_{PA}^{DC}$ ,  $P_{RF}^{DC}$ , and  $P_{BB}^{DC}$  are the power amplifier (PA), radio frequency (RF), and baseband power (BB), respectively. Losses incurred by the DC-DC regulator and active cooling (air conditioner) scale linearly with the power consumption of the other components and may be approximated by loss factors  $\sigma_{DC} = 6\%$ , and  $\sigma_{cool} = 10\%$ . The power consumption of the air-conditioning unit depends on the internal and ambient temperature of the BS cabinet. Typically, an internal and ambient temperature of 25 °C is assumed, resulting in constant power consumption for the air conditioning.  $P_{PA}^{DC}$  is a linear function of the BS transmission power  $P_{tx}^{max}$  and is expressed as  $P_{tx}^{max} / \eta_{PA}$ , where  $\eta_{PA}$  is the PA efficiency. In general, the BS transmission power depends on the radius of coverage and the signal propagation fading. To simplify the model derivation, the macro BS transmission power is normalized as  $P_o = 40$  W with a coverage radius of  $R_o = 1$  km. Similarly, the BS transmission power with coverage radius  $R$  is denoted by  $P_{tx}^{max} = P_o \times (R/R_o)^\alpha$ , where  $\alpha$  is the path loss coefficient. Therefore, the BS operating power with coverage radius  $R$  is expressed as  $P_{op} = N_{TRX} [P_o \cdot (R/R_o)^\alpha / \eta_{PA} + P_{RF}^{DC} + P_{BB}^{DC}] / (1 - \sigma_{DC})(1 - \sigma_{cool})$ . In addition, most sites use a microwave backhaul ( $P_{mc}$ ), and auxiliary equipment located at the BS site include lighting ( $P_{lm}$ ). Then, a mathematical expression for the power consumption of a BS site is given by Equation (1):

$$P_{BS} = \frac{N_{TRX} \left( \frac{P_o \left( \frac{R}{R_o} \right)^\alpha}{\eta_{PA}} + P_{RF}^{DC} + P_{BB}^{DC} \right)}{(1 - \sigma_{DC})(1 - \sigma_{cool})} + P_{mc} + P_{lm} \quad (1)$$

Table 1 summarises the power consumption of the different pieces of LTE-macro BS equipment for a  $2 \times 2$  multiple-input and multiple-output (MIMO) antenna configuration with three sectors.

**Table 1.** Power consumption of the LTE-macro BS hardware elements [21].

Item	Notation	Unit	LTE Macro-BS
PA	Max transmit ( <i>rms</i> ) power, $P_{max}$	W	39.8
	Max transmit ( <i>rms</i> ) power	dBm	46.0
	Peak average power ratio (PAPR)	dB	8.0
	Peak output power	dBm	54.0
	PA efficiency, $\mu$	%	38.8
	Total PA $P_{PA}^{DC} = \frac{P_{max}}{\mu}$	W	102.6
TRX	$P_{TX}$	W	5.7
	$P_{RX}$	W	5.2
	Total RF $P_{RF}^{DC}$	W	10.9
BB	Radio (inner Rx/Tx)	W	5.4
	Turbo code (outer Rx/Tx)	W	4.4
	Processor	W	5.0
	Total BB $P_{RF}^{DC}$	W	14.8
	DC-DC loss, $\sigma_{DC}$	%	6.0
	Cooling loss, $\sigma_{cool}$	%	10.0
	Total per TRX = $\frac{P_{PA}^{DC} + P_{RF}^{DC} + P_{BB}^{DC}}{(1 - \sigma_{DC})(1 - \sigma_{cool})}$	W	151.65

Table 1. Cont.

Item	Notation	Unit	LTE Macro-BS
	Number of sectors ( $N_{Sect}$ )	#	3
	Number of antennas ( $N_{Ant}$ )	#	2
	Number of carriers ( $N_{Carr}$ )	#	1
	Number of transceivers ( $N_{TRX} = N_{Sect} \times N_{Ant} \times N_{Carr}$ )	#	6
Total number of $N_{TRX}$ chains, $P_{op} = N_{TRX} \times$ Total per TRX		W	909.93
	Microwave link ( $P_{mc}$ )	W	80
	Lamps $P_{lm}^{AC}$	W	40

In addition, Figure 3 shows the hourly load profiles. The alternating current (AC) load includes a 91 W air conditioner that represents 10% of  $P_{op}$  and 40 W lighting that operates from 7 PM to 7 AM. The direct current (DC) load includes a BS ( $P_{op}$  minus air conditioner equals 819 W and microwave backhaul equals 80 W).

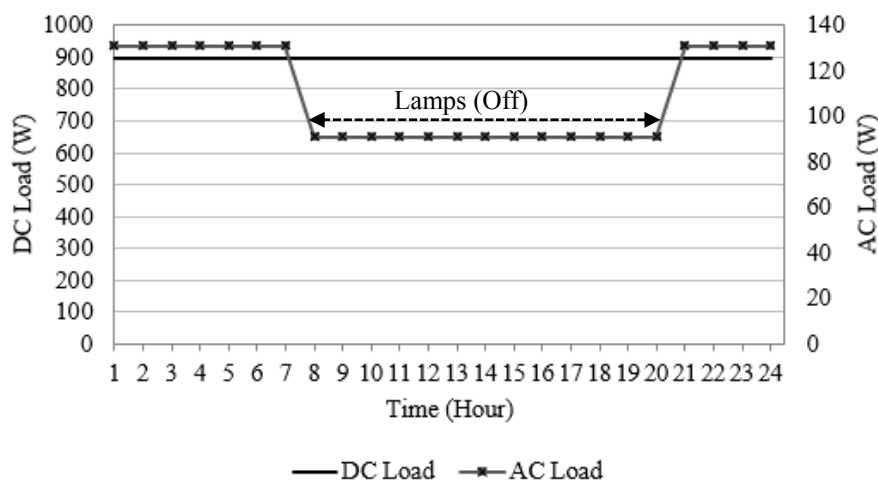


Figure 3. Hourly load profile for the LTE macro-BS.

### 3.2. SPV/WTG Power Subsystem

The solar power supply system consists of various elements (as listed below) that all contribute to energy savings, and have to be designed in a way that allows easy disassembling and component separation for recycling.

- Solar panels: responsible for absorbing shortwave irradiance and converting light into direct current (DC) electricity [23].
- WTG: responsible for converting wind energy to a regulated power which can be connected to the DC-power bus. Generally, for a small power load, vertical style windmills show some special benefit [23].
- Regulator charger: the highest power demand in a typical BS is based on 48 V<sub>dc</sub> voltage. Therefore, it is beneficial to use DC/DC solar regulator converters that can directly convert the unregulated DC output voltage and current from a solar panel to a regulated output voltage for the BS equipment to protect the battery bank.
- Battery bank: stores excess electricity for future consumption by the BS at night, during load-shedding hours or if the available solar energy is not sufficient to feed the BS load completely. To protect the battery, inclusion of a charge controller is recommended. A charge controller or battery regulator limits the rate at which the electric current is added to or drawn from

electric batteries, preventing overcharging and potentially protecting against overvoltage that can reduce battery performance or lifespan and may pose a safety risk. A charge controller may also prevent complete battery draining (“deep discharging”) or perform controlled discharges, depending on the battery technology, to protect battery life [23].

- e. Inverter: An inverter is a device that changes a low DC-voltage into usable 220 V AC voltage. It is one of the system's main elements. Inverters differ by the output wave format, output power and installation type. It is also called a power conditioner because it changes the form of the electric power. There are two types of output wave format: modified sine-wave (MSW) and pure sine-wave. The MSW inverters are economical and efficient; the sine wave inverters are usually more sophisticated with high-end performance that can operate virtually any type of load [23].
- f. Control system: serves as the brains of a complex control, regulation, and communication system. The most common communication units in the remote interface are wireless modems or network solutions. In addition to the control functions, the data logger and alarm memory capabilities are of high importance. All power sources working in parallel are managed by a sophisticated control system and share the load with their capabilities to accommodate the fact that power shortages are not admissible in the cellular telephony sector.

#### 4. Mathematical Model

This section addresses the details of the mathematical model of a hybrid SPV/WTG system proposed to feed the LTE macro-BS.

##### 4.1. Photovoltaic System

The SPV generator contains modules that are composed of many solar cells interconnected in series/parallel to form a solar array. HOMER calculates the energy output of the SPV array ( $E_{PV}$ ) by using the following equation [24],

$$E_{PV} = Y_{PV} \times PSH \times f_{PV} \quad (2)$$

where  $Y_{PV}$  is the rated capacity of the SPV array (kW), and  $PSH$  is a peak solar hour which is used to express solar irradiation in a particular location when the sun is shining at its maximum value for a certain number of hours. Because the peak solar radiation is  $1 \text{ kW/m}^2$ , the number of peak sun hours is numerically equal to the daily solar radiation in  $\text{kWh/m}^2$  [25] and  $f_{PV}$  is the SPV derating factor (sometimes called the performance ratio), a scaling factor meant to account for effects of dust on the panel, wire losses, elevated temperature, or anything else that would cause the output of the SPV array to deviate from the expected output under ideal conditions. In other words, the derating factor refers to the relationship between actual yield and target yield, which is called the efficiency of the SPV. Today, due to improved manufacturing techniques, the performance ratio of solar cells increased to 85%–95%.

##### 4.2. Wind Conversion System

This system produces energy by converting the flowing wind speed into mechanical energy and then into electricity. The power contained in the wind kinetic energy is expressed by [24]:

$$P = \frac{1}{2} \rho V^3 C_p \quad (3)$$

where  $V$  is the monthly wind speed (m/s),  $C_p$  is the coefficient of the Betz limit, which can achieve a maximum value of 59% for all types of wind turbines, and  $\rho$  is the corrected monthly air density ( $\text{kg/m}^3$ ). HOMER assumes that the power curve applies a standard air density of  $1.225 \text{ kg/m}^3$ , which corresponds to standard temperature and pressure conditions.

### 4.3. Battery Model

The battery characteristics that play a significant role in designing a hybrid renewable energy system are battery capacity, battery voltage, battery state of charge, depth of discharge, days of autonomy, efficiency, and lifetime of battery.

The nominal capacity of the battery bank is the maximum state of charge  $SOC_{max}$  of the battery. The minimum state of charge of the battery,  $SOC_{min}$ , is the lower limit that does not discharge below the minimum state of charge. The  $DOD$  is used to describe how deeply the battery is discharged and is expressed in Equation (4) [24]:

$$DOD = 1 - SOC_{min} \quad (4)$$

Based on Equation (4), the  $DOD$  for the “Trojan L16P” battery is 70%, which means that the battery has delivered 70% of its energy and has 30% of its energy reserved.  $DOD$  can always be treated as how much energy the battery delivered. A battery bank is used as a backup system and is sized to meet the load demand when the renewable energy resources failed to satisfy the load. The number of days a fully charged battery can feed the load without any contribution of auxiliary power sources is represented by days of autonomy. The battery bank autonomy is the ratio of the battery bank size to the electric load (LTE-macro BS). HOMER calculates the battery bank autonomy ( $A_{batt}$ ) by using the following equation [24]:

$$A_{batt} = \frac{N_{batt} \times V_{nom} \times Q_{nom} \left(1 - \frac{SOC_{min}}{100}\right) (24 \text{ h/d})}{L_{prim-avg} (1000 \text{ Wh/kWh})} \quad (5)$$

where  $N_{batt}$  is the number of batteries in the battery bank,  $V_{nom}$  is the nominal voltage of a single battery (V),  $Q_{nom}$  is the nominal capacity of a single battery (Ah), and  $L_{prim,ave}$  is the average daily LTE-macro BS load (kWh). Battery life is an important factor that has a direct impact on replacement costs. Two independent factors may limit the lifetime of the battery bank: the lifetime throughput and the battery float life. HOMER calculates the battery bank life ( $R_{batt}$ ) based on these two factors as given in the following equation [24]:

$$R_{batt} = \min \left( \frac{N_{batt} \times Q_{lifetime}}{Q_{thrpt}}, R_{batt,f} \right) \quad (6)$$

where  $Q_{lifetime}$  is the lifetime throughput of a single battery (kWh),  $Q_{thrpt}$  is the annual battery throughput (kWh/year), and  $R_{batt,f}$  is battery float life (year).

### 4.4. Economic Mathematical Model

HOMER calculates the net present cost (NPC) according to the following equation [24]:

$$NPC = \frac{TAC}{CRF} \quad (7)$$

where  $TAC$  is the total annualised cost (\$). The capital recovery factor (CRF) is given by [24],

$$CRF = \frac{i(1+i)^n}{(1+i)^n - 1} \quad (8)$$

where  $n$  is the project life time, and  $i$  is the annual real interest rate. HOMER assumes that all prices escalate at the same rate and applies an annual real interest rate rather than a nominal interest rate.

The discount factor ( $f_d$ ) is a ratio used to calculate the present value of a cash flow that occurs in any year of the project lifetime. HOMER calculates the discount factor by using the following equation [24]:

$$f_d = \frac{1}{(1+i)^n} \quad (9)$$

NPC estimation in HOMER also considers the salvage cost, which is the residual value of the power system components at the end of the project lifetime. The equation used to calculate the salvage value ( $S$ ) [24] is:

$$S = rep \left( \frac{rem}{comp} \right) \quad (10)$$

where  $rep$  is the replacement cost of the component,  $rem$  is the remaining lifetime of the component, and  $comp$  is the lifetime of the component.

## 5. System Implementation and Configuration

The implementation of a hybrid SPV/WTG system within the HOMER software and the configurations for the various elements in the system are given in Figure 4.

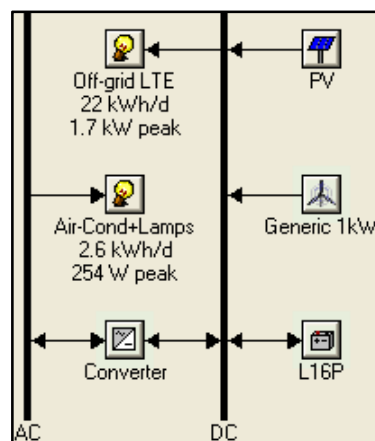


Figure 4. Micro-power system modelling in HOMER.

HOMER model the operation of a system by generating energy balance calculations for each of the 8760 h in a year. For every hour, HOMER compares the electric demand of BS in one hour to the energy that the system can supply in that hour, calculates the energy flows to and from each component of the system, and determines whether to charge or discharge the batteries. The model then decides whether or not a configuration is feasible, i.e., whether it can meet the electric demand under the specified conditions, and estimates the cost of installing and operating the system throughout the lifetime of the project. Figure 5 summarizes the main parts of HOMER simulation, inputs, optimization, and outputs; to finding the best optimized system with low NPC. To perform simulation and optimisation of a power system using the HOMER tool, information and data on natural resources (wind speed and solar irradiance data), LTE BS load, economic constraints (real interest rate), equipment costs and lifetime, project lifecycle are required, which will provide in the following subsections.

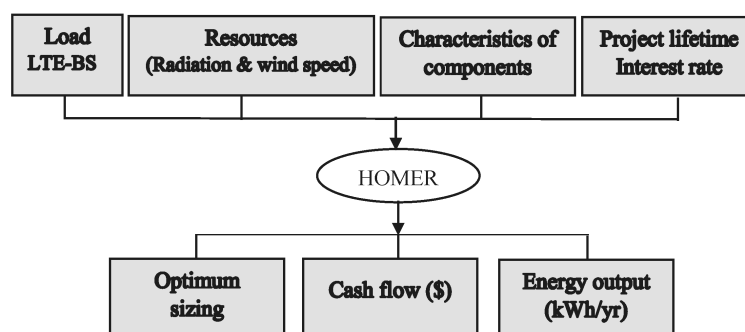


Figure 5. Architecture of HOMER software.

### 5.1. Solar Radiation

The monthly average solar radiation values used in this study are obtained based on both the Korea Meteorological Administration (KMA) and the NASA Surface Meteorology and Solar Energy using the longitude and latitude of South Korea [26,27].

The average daily solar radiation in South Korea, which is located at a latitude between 34° and 38° north, is estimated to be 4.01 kWh/m<sup>2</sup> and varies from 2.474 kWh/m<sup>2</sup> in December to 5.622 kWh/m<sup>2</sup> in May [26,27]. The monthly variation, as shown in Figure 6, is largely due to the shift in the elevation angle of the sun.

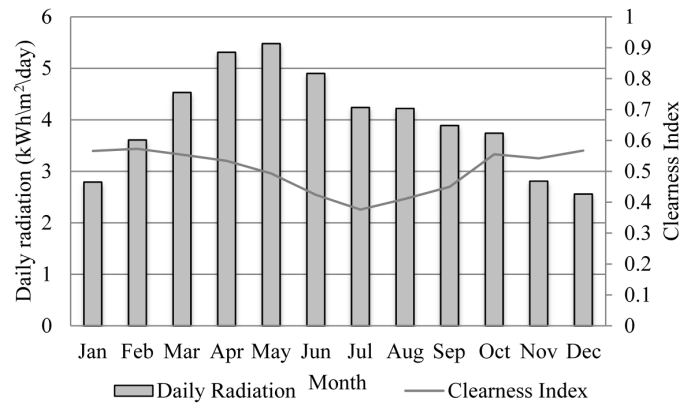


Figure 6. Monthly average solar global horizontal irradiance at 35.5° latitude and 127.5° longitude [26,27].

Moreover, solar radiation in different areas of South Korea is shown in Figure 7. Relatively higher solar radiation of over 5 kWh/m<sup>2</sup>/day can be obtained in the southwestern coastal area including Jeju island. In contrast, in the northwestern region around Seoul, solar radiation is lowered to approximately 4.7 kWh/m<sup>2</sup>/day, and Gochang, located at the western coast of South Korea, shows the lowest solar radiation of 4.48 kWh/m<sup>2</sup>/day. Accordingly, this study will investigate different values of average daily solar radiation values to cover all of the areas of South Korea: 4.0, 4.5, 5.0, and 5.5 kWh/m<sup>2</sup>.

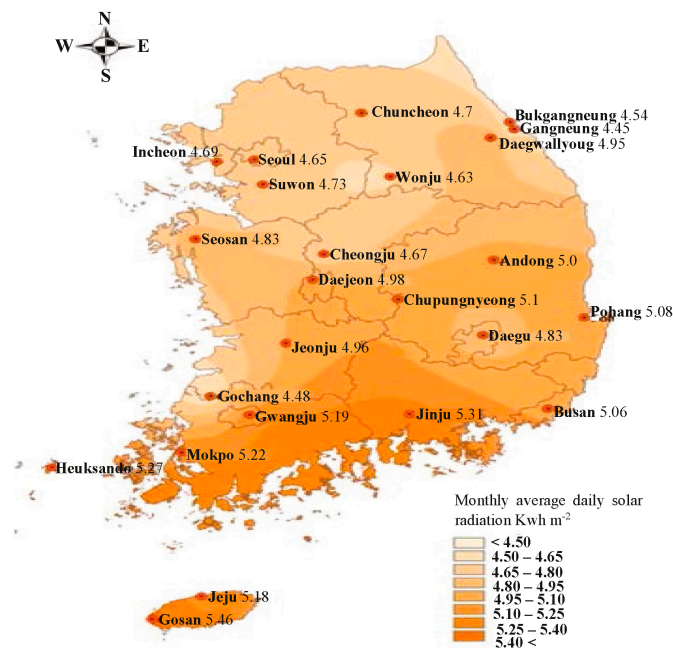


Figure 7. Monthly average daily solar radiation [28].

## 5.2. Wind Speed

The wind energy resource data used in this paper was mainly obtained from the Weather Resource Maps of the National Institute of Meteorological Science (NIMS). Figure 8 shows the average wind speed at 50 m above the surface of the earth in South Korea [29]. The average wind speed in the most of the interior of South Korea does not exceed 4 m/s. However, the wind speed above 7.5 m/s can be observed in the mountainous regions nearby east coast, the southeastern coast, and Jeju Island which is located at the below of the peninsula. In particular, almost every region in Jeju Island shows the wind speed above 5.5 m/s, which is the main reason why a lot of wind turbines have been installed in Jeju Island.

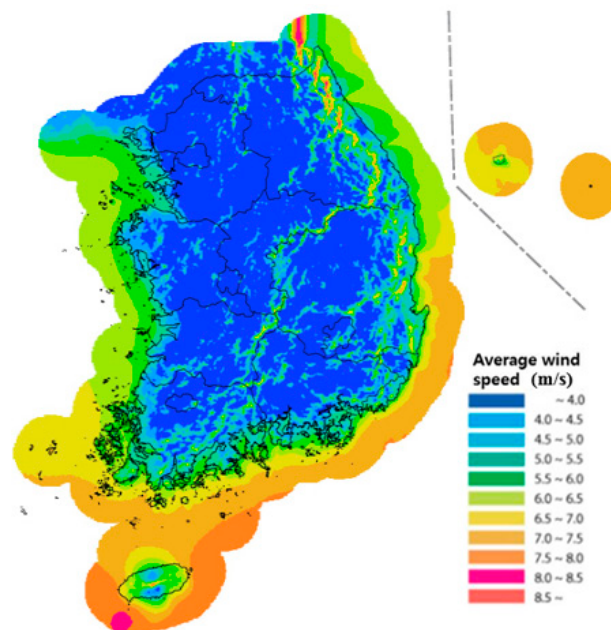


Figure 8. Average wind speed in South Korea [29].

The monthly average wind speed for South Korea is shown in Figure 9 [26,27]. In summer the wind speed considerably decreases compared with the wind speed in winter. This seasonal variation of the wind speed is deeply related with the atmospheric pressure around South Korea and finally the direction of the wind. In summer the North Pacific atmospheric pressure is to the south of South Korea and affects to every region in South Korea. This causes the direction of the wind in summer is largely southeast or southwest. On the contrary, the northwestern wind is mainly occurred in winter, which is originated from the high Siberia atmospheric pressure located on the north of South Korea. The change of the wind direction with the season is one of the weak points for using the wind energy in South Korea.

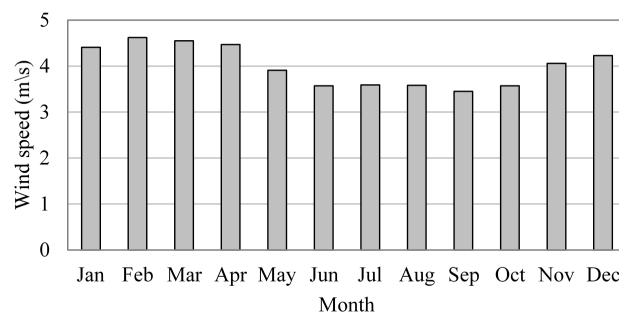
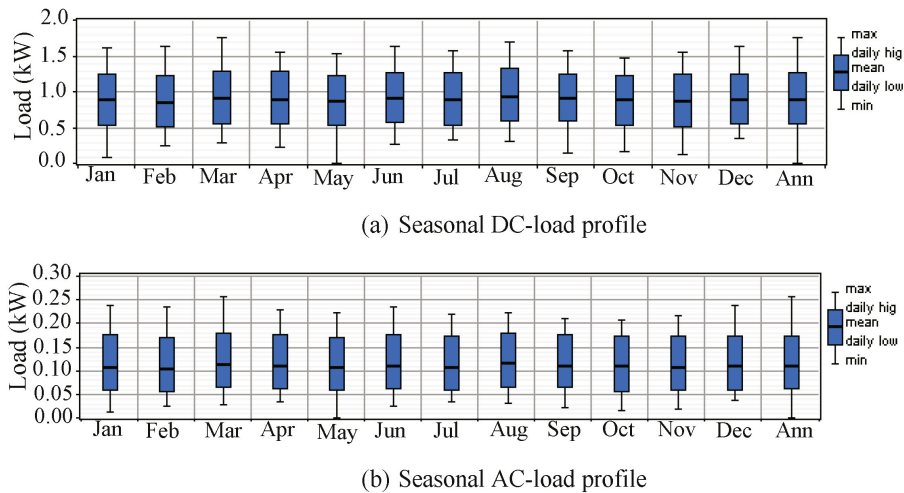


Figure 9. Monthly average wind speed for South Korea [26,27].

### 5.3. Load Profile

The LTE-macro BS load is critical for designing a reliable and efficient system. Sizing and modelling of the solar power system depend on the load profile. We used 24-hour load values for 365 days for an accurate analysis. The seasonal load profiles for both the DC and AC loads are shown in Figure 10.



**Figure 10.** Seasonal load profiles: (a) DC-load profile; (b) AC-load profile.

### 5.4. Technical and Economic Criteria of the SPV/WTG System

The control parameters and the technical and economic criteria of the SPV/WTG system's components are provided in the following subsections.

#### 5.4.1. Annual Real Interest Rate and Project Lifetime

The South Korea annual real interest rate was 1.25% in June 2016 [30]. However, the lifetime of the project is 10 years, representing the lifetime of the BS equipment [31].

#### 5.4.2. SPV

The "Sharp" solar model is considered in this study; this model has highly efficient, affordable systems. Moreover, the Sharp solar module incorporates an advanced surface to increase light absorption and improve efficiency [32]. The technical specifications and costs used in the HOMER simulation based on the proposed solar model are listed below:

- Economic issues: the initial installation costs of SPV, the replacement costs, and the annual O&M costs per 1 kW are \$1000, \$1000, and \$10, respectively.
- Technical issues: the lifetime of an SPV array is 25 years; a derating factor of 0.9, a reflectance of 20%, and a dual-axis tracking system for the SPV array are used in this paper.
- SPV size: the sizes of the simulation values of the applied SPV panels are 4, 4.5, 5, 5.5, 6, 6.5, and 7 kW.

#### 5.4.3. WTG

The FT-1000L WTG model is considered in this study; this model is affordable [33]. In addition, Figure 11 summarises the output power at different wind speed values. The technical specifications and costs used in the HOMER simulation are based on the proposed WTG model and are listed below:

- Economic issues: the initial installation costs of a WTG, the replacement costs, and the annual O&M costs per 1 kW are \$600, \$600, and \$50, respectively.

- b. Technical issues: the lifetime of a WTG and the height of the hub are 15 years and 50 m, respectively.
- c. WTG size: the sizes of the simulation values of the applied WTG are 1, 2, and 3 kW.

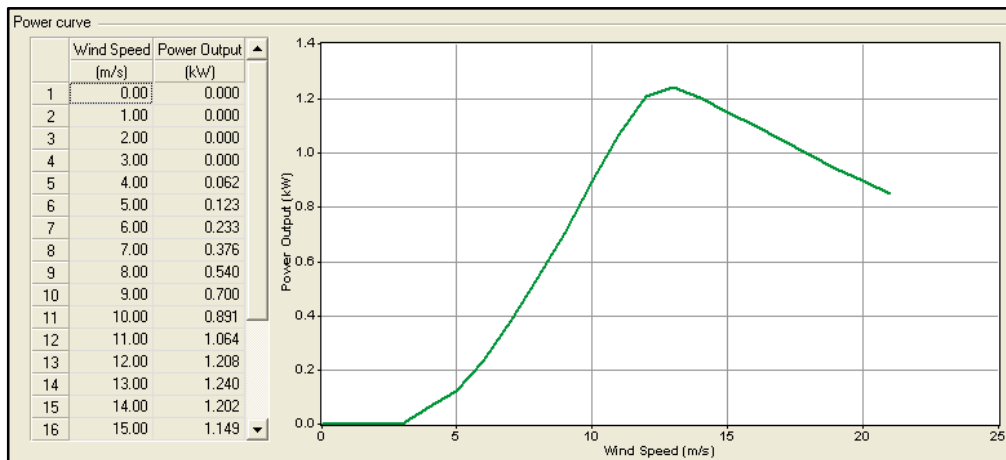


Figure 11. The output power over a different wind speed values.

#### 5.4.4. Battery

The “Trojan L16P” battery model is considered in this study, which provides good characteristics combined with low cost. Figure 12 summarises the technical specifications to “Trojan L16P” battery model. More details can be found in [34]. The technical specifications and costs used in the HOMER simulation based on the proposed battery model are listed below:

- a. Economic issues: the initial installation costs of a battery, the replacement costs, and the annual O&M costs per unit are \$300, \$300, and \$10, respectively.
- b. Technical issues: the lifetime of the “Trojan L16P” battery and the efficiency are set as 5 years and 85%, respectively.
- c. Battery size: the sizes of the simulation-values of the applied inverter are 32, 40, 48, 56, 64 and 72 units.

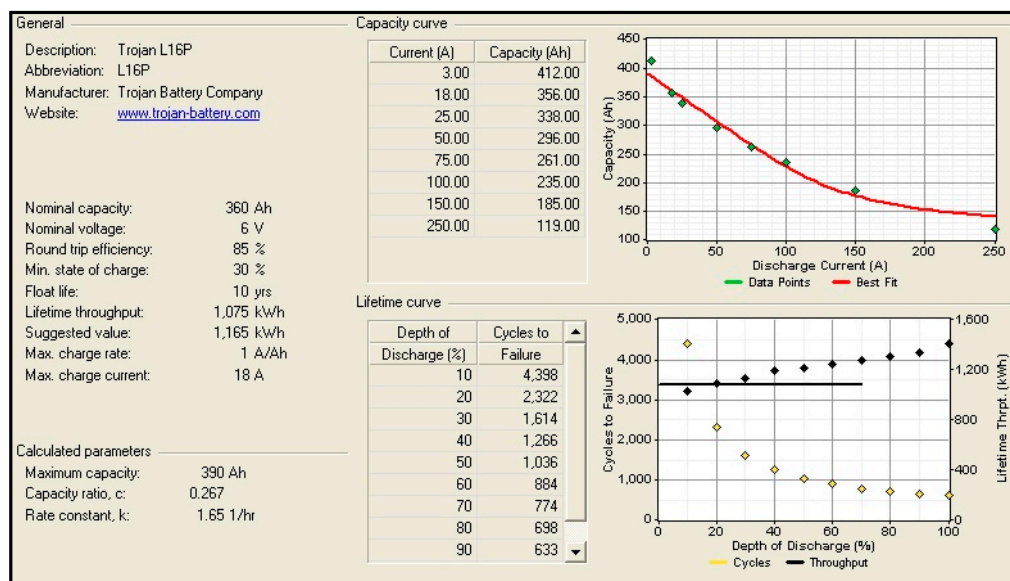


Figure 12. “Trojan L16P” battery model characteristics.

## 5.4.5. Inverter

- Economic issues: the initial installation costs of an inverter, the replacement costs, and the annual O&M costs per 1 kW are \$400, \$400, and \$10, respectively.
- Technical issues: the lifetime of the inverter, and the efficiency are set as 15 years, 95%, respectively.
- Inverter size: the sizes of the simulation-values of the applied inverter are 0.1, 0.15, 0.2, 0.25, and 0.3 kW.

Moreover, the technical specifications, costs, economic parameters, and system constraints that are used in the present study are summarized in Table 2 below.

**Table 2.** HOMER simulation setup.

System	Parameters	Value
Renewable energy resources	Solar radiation	4.0, 4.5, 5.0, 5.5 kWh/m <sup>2</sup> /day
	Wind speed	4.0 m/s
Control parameters	Annual real interest rate	1.25%
	Project lifetime	10 years
	Dispatch strategy	cyclic charging
	Apply setpoint state of charge	80%
	Operating reserve: as percent of load, hourly load	10%
SPV	Sizes considered	4, 4.5, 5.5, 6, 6.5, 7 kW
	Operational lifetime	25 years
	Efficiency	90%
	System tracking	Two axis
	Capital cost	\$1/W
	Replacement cost	\$1/W
	O&M cost per year	\$0.01/W
WTG	Sizes considered	1, 2, and 3 kW
	Operational lifetime	15 years
	Hub	50 m
	Capital cost	\$0.6/W
	Replacement cost	\$0.6/W
	O&M cost per year	\$0.05/W
Inverter	Sizes considered	0.1, 0.15, 0.2, 0.25, & 0.3 kW
	Efficiency	95%
	Operational lifetime	15 years
	Capital cost	\$0.4/W
	Replacement cost	\$0.4/W
	O&M cost per year	\$0.01/W
Trojan L16P Battery	Number of batteries	32, 40, 48, 56, 64, 72
	Round trip efficiency	85%
	Minimum state of charge	30%
	Nominal voltage	6 V
	Nominal current	360 Ah at 20 h
	Nominal capacity	6 V × 360 Ah = 2.16 kWh
	Lifetime throughput	1075 kWh
	Max. charge rate	1 A/Ah
	Max. charge current	18 A
	Self-discharge rate	0.1% per hour
	Min. operational lifetime	5 years
	Capital cost	\$300
	Replacement cost	\$300
	O&M cost per year	\$10

## 6. Optimization and Simulation Results

Different average daily solar radiation values of 4.0, 4.5, 5.0 and 5.5 kWh/m<sup>2</sup> are used to simulate the application of solar energy across a wide range of South Korea areas (as shown in Figure 7)

with 4.0 m/s wind speed. Additional configuration details are given in Table 2. The energy output, the economic analysis of the proposed hybrid power system, and the related sensitivity analysis are provided in the following paragraphs.

### 6.1. Optimisation Criteria

Table 3 includes a summary of the economic and technical criteria for an optimal design of the SPV/WTG system based on different values of solar radiation and a 4.0 m/s wind speed.

**Table 3.** SPV/WTG system: optimal sizing and economic criteria.

Resources		Optimum Sizing				Costs Factor		
Wind Speed (m/s)	Radiation (kWh/m <sup>2</sup> /day)	SPV (kW)	WTG (kW)	Battery (unit)	Inverter (kW)	Initial Cost (IC) (\$)	Annual O&M (\$)	NPC (\$)
4.0	4.0	6.0	1	64	0.20	25,880	752	29,528
	4.5	5.0	1	64	0.20	24,880	742	28,965
	5.0	4.5	1	64	0.20	24,380	737	28,683
	5.5	4.0	1	64	0.20	23,880	732	28,401

Table 3 indicates that the size of the SPV array decreases with increasing solar radiation. In contrast, the size of the WTG is 1 kW for all solar radiation cases because the wind speed is constant at 4.0 m/s. The optimal number of batteries, which was found by the HOMER simulation for the system, is 64 batteries. In addition, the inverter (DC/AC) needed must be capable of handling 0.2 kW.

The SPV array, which is a 20 Sharp ND-F4Q300 module (polycrystalline), is rated at 6.0 kW with a voltage  $V_{pm}$  of 35.20  $V_{dc}$ , a current  $I_{pm}$  of 8.52 A, and a power  $P_{pm}$  of 300 W. A 20 Sharp ND-F4Q300 module will be connected with four in series and five in parallel to be compatible with the specifications of the solar control regulator chosen in this study, the Solarcon SPT-4830 [35]. This requires that the open circuit voltage for a SCR  $V_{oc}^{SPT-4830}$ , 192  $V_{dc}$ , be higher than the open circuit voltage of the SPV panel, 180.4  $V_{dc}$  (four SPV modules in series  $\times V_{oc}^{ND-F4Q300}$ , 45.10  $V_{dc}$ ). In addition, the current for a SCR  $I^{SPT-4830}$  must be higher than the short circuit current of the SPV panel  $I_{sc}^{ND-F4Q300}$ , 8.94 A  $\times$  1.3 (safety factor). The optimal size of the WTG was found by the HOMER simulation to be 1 kW; the FT-1000L WTG model is a good choice. The nominal voltage of the *Trojn L16P* battery [31] is 6  $V_{dc}$ , and the nominal capacity is 360 Ah. Thus, the optimal number of batteries (64 batteries) found by the HOMER simulation for the system will be connected with eight in series and eight in parallel because the DC bus-bar is 48  $V_{dc}$ . A typical daily AC load is (air conditioner 91 W + lamps 40 W). Therefore, the inverter must be capable of handling 0.2 kW. *SU200P*, which has specifications of 200 W, an input voltage of 12/24/48  $V_{dc}$ , an output voltage of 220/110  $V_{ac}$ , an AC output frequency of 50 Hz/60 Hz, and a pure sine wave can be chosen.

The system costs consist of the following: (i) the IC cost is paid at the beginning of the project and decreases with decreasing size of the elements of the project; (ii) The operating cost is paid annually, and most of this cost goes towards operating and maintaining the battery bank; (iii) The NPC represents all costs that occur within the project lifetime, including IC costs, component replacements within the project lifetime and O&M costs. Table 3 indicates that the IC and O&M costs decrease with increasing solar radiation because the SPV array size decreases, reducing the total cost (NPC) of the hybrid SPV/WTG system.

### 6.2. Energy Yield Analysis

Figure 13 summarises the annual energy contributions of different sources for different average daily solar radiation values at a wind speed of 4.0 m/s. The energy delivered to the SPV array load depends on the value of solar radiation and the size of the SPV array. However, the energy delivered to the load of the WTG is the same because the optimal WTG size is fixed.

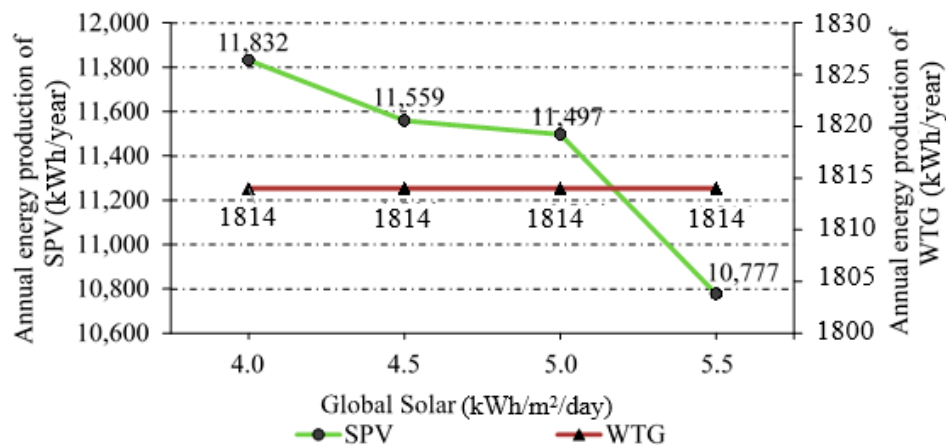


**Figure 13.** Annual energy contribution of different sources with different average solar radiation values and 4.0 m/s wind speed.

The following statistical analysis discusses the energy production based on the average daily solar radiation (4.0 kWh/m<sup>2</sup>) and wind speed (4.0 m/s) for South Korea as a case study. However, this analysis can be extended to other cases, yielding a slight difference in daily peak solar hours per case depending on the average daily solar radiation.

The annual energy contribution of the SPV array is computed based on Equation (2), SPV rated capacity is 6.0 kW × PSH 4.01 h × SPV derating factor 0.9 × 365 days/year, which equals 7904 kWh. However, the tracking system plays a role in increasing the total amount of energy produced by a SPV array. The present simulation adopted a dual axis tracker that increased the total amount of energy to 11,832 kWh. Each hour, HOMER calculates the power output of the wind turbine in a four-step process. First, it determines the average wind speed for the hour at the anemometer height by referring to the wind resource data. Second, it calculates the corresponding wind speed at the turbine’s hub height using either the logarithmic law or the power law. Third, it refers to the turbine’s power curve to calculate the turbine’s power output at that wind speed assuming standard air density. Fourth, it multiplies that power output value by the air density ratio, which is the ratio of the actual air density to the standard air density [21]. The annual energy contribution of the WTG is 1814 kWh. In addition, Figure 14 shows the monthly statistics of the output power for the WTG. It is clear that the maximum energy contribution of the WTG occurred at the first three months of the year (January–March) and at the end two months of the year (November - December), due to decreased the sunshine hours and solar radiation (as shown in Figure 6).

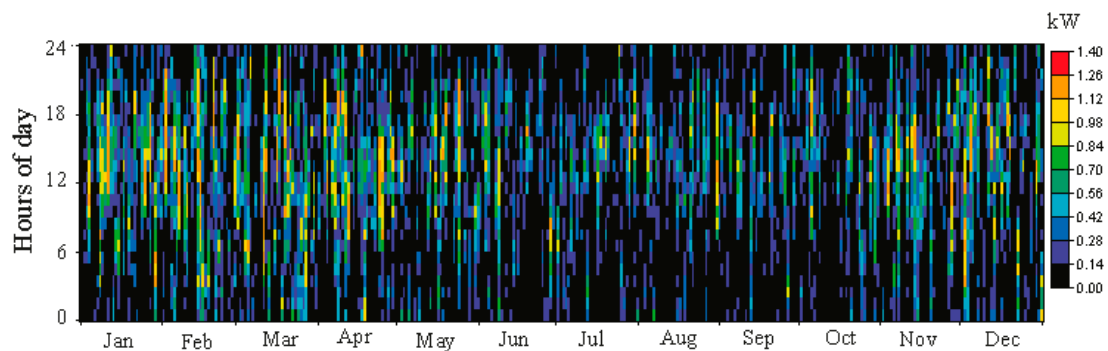
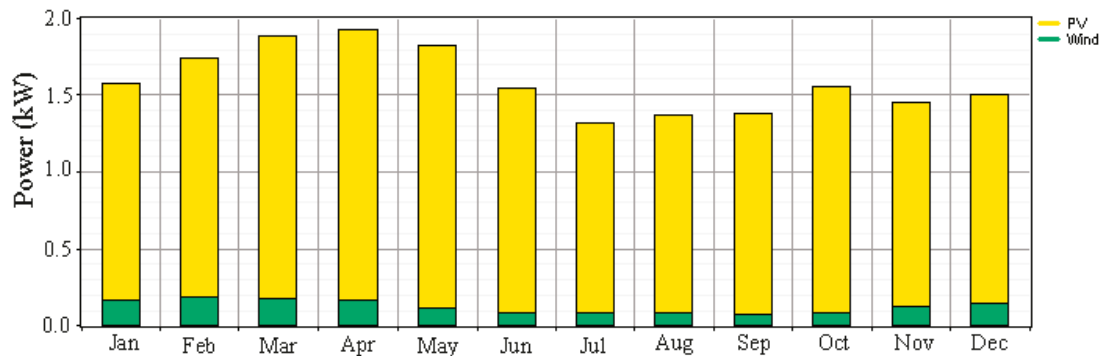


**Figure 14.** Monthly statistics of the WTG output power.

The total annual energy production of the hybrid SPV/WTG system is 13,646 kWh (87% from the SPV array and 13% from the WTG), while the total annual energy needed by an LTE-macro BS

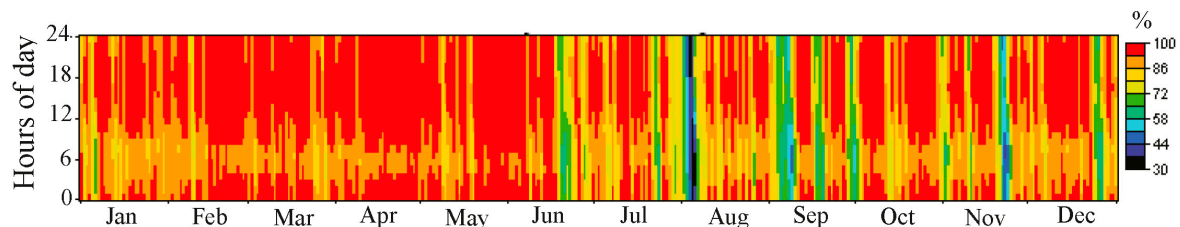
is 8840 kWh, the AC load (air conditioner 91 W + lamps 40 W, operating 7 PM–7 AM) plus the DC load (BS 819 W + microwave link 80 W) multiplied by (24 h × 365 days/year). The difference between electrical production and consumption is equal to the excess electricity of 4004 kWh/year, plus the battery losses of 753 kWh/year, plus inverter losses of 50 kWh/year.

Figure 15 shows the monthly average electric production of the different power sources. The maximum energy contribution of the SPV array occurred in April and May. Meanwhile, the minimum energy contribution occurred in July. These results are attributed to the differences in the average solar radiation rate, as shown in Figure 6. While, the maximum energy contribution of the WTG occurred in February; and the minimum energy contribution occurred in September.



**Figure 15.** Monthly power contribution of various sources at an average solar irradiation  $4.0 \text{ kW/m}^2/\text{day}$  and average wind speed  $4.0 \text{ m/s}$ .

The optimal number of batteries, which was found by the HOMER simulation for the system is 64 battery. The battery annual energy-in is 5162 kWh, while the annual energy-out is 4409 kWh, where the roundtrip efficiency was 85%. Batteries can supply LTE-macro BS load autonomy for 95.9 h (3 days and 23.9 h), which is computed based on Equation (5), (number of the batteries is  $64 \times$  nominal voltage of a single battery  $6 \text{ V} \times$  nominal capacity of a single battery  $360 \text{ Ah} \times$  DOD  $0.7 \times 24 \text{ h}$ ) divided by (daily average LTE-macro BS load  $24.22 \text{ kWh}$ ). However, one battery can supply LTE-macro BS load autonomy 1.5 h. The battery expected life is 10 years, which is computed based on Equation (6). In addition, the seasonal statistics of the maximum and minimum states of charge (SOCs) for the battery are given in Figure 16 and reveal that the highest energy contribution of the battery bank occurred at the end of July because the minimum energy contribution of the hybrid power system occurred in July, as shown in Figure 15.



**Figure 16.** Monthly statistics of the SOC for the battery.

The inverter annual energy-in is 1005 kWh, while the annual energy-out is 955 kWh, based on the daily AC load needs  $2.62 \text{ kWh} \times 365 \text{ days/year}$ , with 95% efficiency and 8759 h/year operation (operating hours  $24 \text{ h} \times 365 \text{ days/year}$ ). Figure 17 shown the monthly statistics of the output power for the inverter, which indicate that the inverter is operating normally.

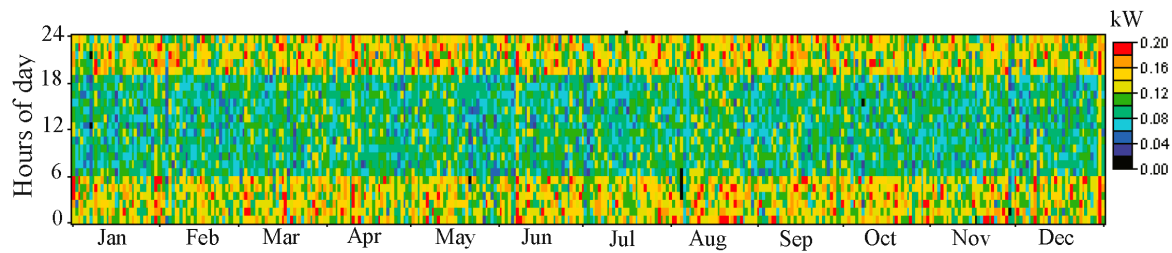


Figure 17. Monthly statistics of the inverter output power.

### 6.3. Economic Analysis

The cash flow summary of the hybrid power system within the project lifetime based on the average daily solar radiation ( $4.0 \text{ kWh/m}^2$ ) and wind speed ( $4.0 \text{ m/s}$ ) for South Korea as a case study is given in Figure 18. However, this analysis can be extended to other cases. The breakdown for the IC, replacement, O&M and salvage costs incurred within the project lifetime is given in the following paragraphs.

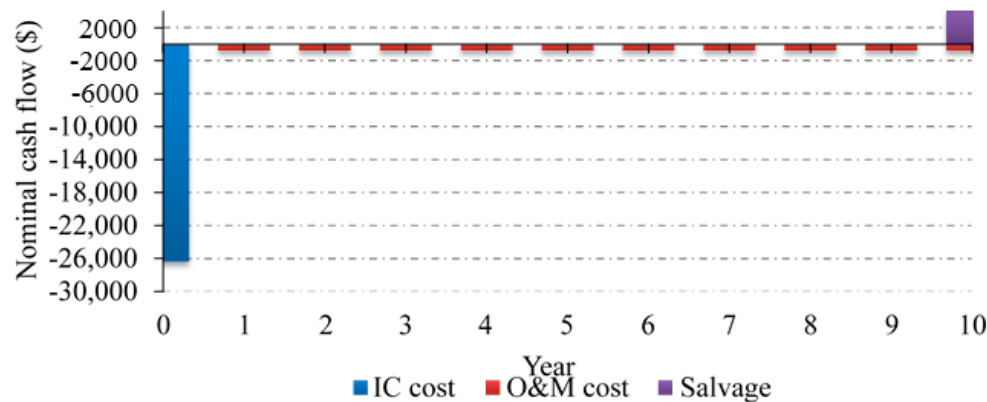


Figure 18. Cash flow summary within the project lifetime.

The *IC cost*, paid once at the beginning of the project, is directly proportional to the size of the system. From Table 3, the IC cost is \$25,880. The breakdown of this cost is as follows: (i) For the SPV (size  $6.0 \text{ kW} \times \text{cost } \$1000/1 \text{ kW} = \$6,000$ ); (ii) for the WTG (size  $1 \text{ kW} \times \text{cost } \$600/1 \text{ kW} = \$600$ ); (iii) for the battery units ( $64 \text{ unit} \times \text{cost } \$300/\text{unit} = \$19,200$ ); and (iv) for the inverter (size  $0.2 \text{ kW} \times \text{cost } \$400/1 \text{ kW} = \$80$ ).

The annual *O&M costs* of the hybrid power system amounted to \$752. The breakdown of this cost is as follows: (i) for the SPV (size  $6.0 \text{ kW} \times \$10/1 \text{ kW} = \$60$ ); (ii) for the WTG (size  $1 \text{ kW} \times \$50/1 \text{ kW} = \$50$ ); (iii) for the battery units ( $64 \text{ unit} \times \$10/\text{unit} = \$640$ ); and (iv) for the inverter ( $0.2 \text{ kW} \times \text{cost } \$10/1 \text{ kW} = \$2$ ).

It is clear that the battery bank represents the bulk of both the IC and O&M costs. However, this cost depended on the number of batteries in the system. Herein, the optimal number of batteries was determined by HOMER to be 64 battery; the number of batteries can be reduced. However, the load autonomy decreases, which is considered to be an important issue, especially in remote rural areas.

The batteries have a lifetime of 10 years, which is the same as the project lifetime; the SPV array has a lifetime of 25 years, and the WTG has a lifetime of 15 years. Thus, neither requires replacement.

Each component has a *salvage value* at the end of the project lifetime. The SPV array salvage value is \$3600, the highest in the system, which was computed based on Equation (10), (SPV array remaining lifetime (15)/SPV array lifetime (25)) multiplied by the replacement cost of the SPV array, \$6000. While,

the WTG salvage value is \$200 the inverter salvage value is \$27. Thus, the total salvage value at the end project lifetime is \$3827.

The economic analysis described above has been conducted on the basis of the nominal system. However, Figure 19 showed the discount factor for each year of the project lifetime, which computed based on Equation (9).

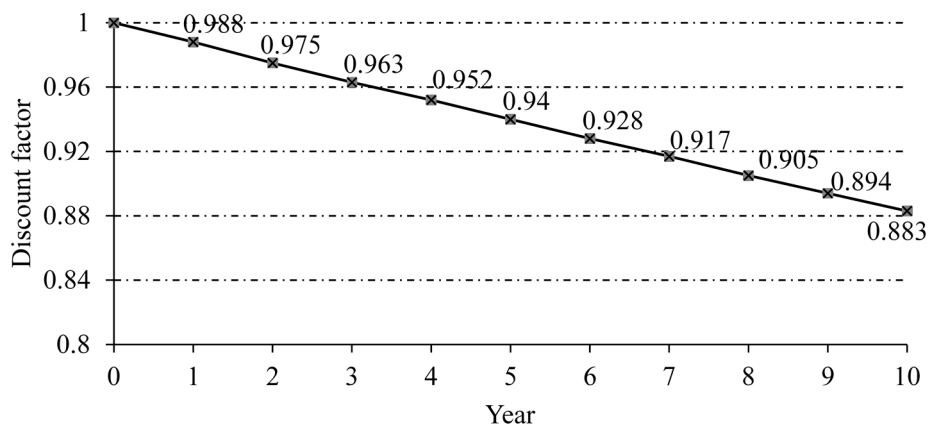


Figure 19. Discount factor for each year of the project lifetime.

The total NPC calculates by summing up the total discounted cash flows in each year of the project lifetime, as follows: include capital costs \$25,880 + O&M costs \$7075 – salvage \$3645, equal \$29,810. This analysis can be extended to other cases in which the cost of the system depends on the elements and the size of the components in the system. Figure 20 summarized the total discounted costs occurring within the project lifetime for the hybrid SPV/WTG system.

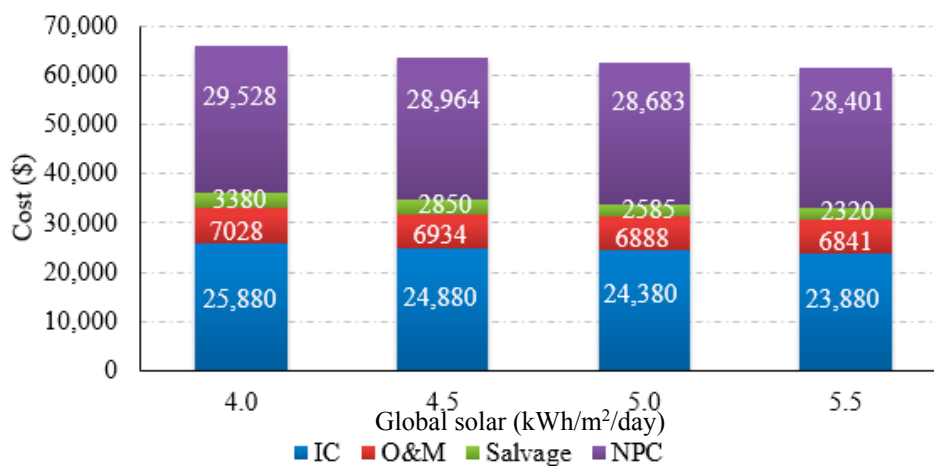


Figure 20. Summary of all costs occurring within the project lifetime for the SPV/WTG hybrid system.

### 7. Comparison of the Feasibility of Using a Hybrid SPV/WTG system vs. a Diesel Generator

The comparison between the traditional power system DG and the proposed SPV/WTG system is summarized into two important key aspects: (i) economic feasibility and (ii) greenhouse gases (GHG) emissions. The following discussion is based on an average daily solar radiation for South Korea of 4.0 kWh/m<sup>2</sup> and a wind speed of 4.0 m/s as a case study. However, this discussion can be extended to include other cases of solar radiation, with a slight difference in the IC, O&M, and salvage costs.

### 7.1. Diesel Generator

The DG needed approximately is 4 kW, which computed as (maximum LTE-macro BS, AC and DC load 1.1 kW) divided by (DG efficiency 30% [7]  $\times$  converter efficiency 95%):

- i. IC cost: the DG IC cost is \$2640 (size 4 kW  $\times$  cost \$660/1 kW). However, the fossil fuels not sustainable and expensive, and the price go up continuously.
- ii. O&M cost: the annual cost for the maintenance and operation of the DG amounted to \$4680 (without counting the cost of fuel transport). A breakdown of this cost, (i) \$438 for DG maintenance per year based on a DG maintenance cost of \$0.05/h  $\times$  annual DG operating hours 8760 h; and (ii) a fuel cost of \$4242, based on the diesel price of \$1.04/L [36]) multiplied by the a total diesel consumption of 4079 L per year, which computed based on a specific fuel consumption of 0.388 L/kWh  $\times$  annual electrical production of the DG of 10,512 kWh/year (DG capacity size 4 kW  $\times$  DG efficiency 0.3  $\times$  24 h  $\times$  365 days/year).
- iii. Replacement cost: mobile operator may need to change the DG every 3 years, which means at least three times during the life of the project. Thus, the total DG replacement cost is 3  $\times$  (size 4 kW  $\times$  cost \$660/1 kW), equal \$7920 at least.
- iv. NPC cost: the total NPC include IC cost \$2640 + O&M cost \$46,800 + Replacement cost \$7920, equal \$57,360 over the project lifetime (10 years); without counting the cost of fuel transport, which adds further to this cost.
- v. GHG emissions: According to [37], the CO<sub>2</sub> emissions of diesel fuel are 2.68 kg/L. Hence, the total annual CO<sub>2</sub> emissions are 10,931 kg, computed based on the specific annual diesel consumption of 4079 L multiplied by 2.68 kg CO<sub>2</sub>/L.

### 7.2. Hybrid SPV/WTG System

- i. IC cost: the hybrid SPV/WTG system IC cost is \$25,880. The IC cost of the SPV/WTG system is high, due to that the components of the system are expensive comparing with DG. However, the global price of SPV/WTG system go down continuously.
- ii. O&M cost: by applying the proposed SPV/WTG system; a large benefits for mobile operators can be achieved for long term. Since the annual O&M cost can be decreasing to \$752, which mean saving amounted 83.83% comparing with O&M cost for DG. However, savings rate will increase more and more in the future, due to the continuing rise in fuel prices.
- iii. Replacement cost: by applying the proposed SPV/WTG system, the batteries have a lifetime of 10 years, which is the same as the project lifetime, the SPV array has a lifetime of 25 years, and WTG and inverter have has a lifetime of 10 years, so neither requires replacement.
- iv. NPC cost: the total NPC include capital costs \$25,880 + O&M costs \$7028 – salvage \$3380, equal \$29,528 over the project lifetime (10 years).
- v. GHG emissions: Renewable energy systems (RESs) are considered an icon of all that is green. Hence, the trend towards RESs is increasing all over the world to eliminate GHG emissions and minimise the effect on both the wallet and the environment.

By applying the proposed SPV/WTG system, the total NPC that can be saving amounted up to 48.52%. Figure 21 summarized OPEX of the traditional power system (DG only) compare with the proposed SPV/WTG system over the project lifetime (10 years).

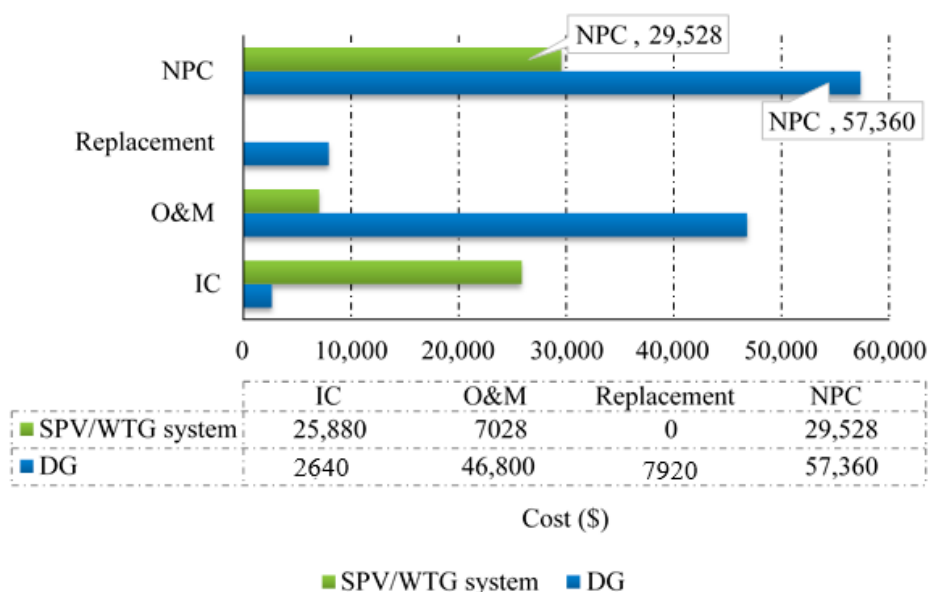


**Figure 21.** Summary an OPEX of the SPV/WTG system vs. DG over the project lifetime.

## 8. Conclusions

Providing a reliable, secure power and energy system is one of the main issues in cellular networks. Accordingly, this study examined supplying LTE-macro BSs the needed energy by a hybrid SPV with a WTG power system. Three key aspects have been discussed: (i) optimal system architecture; (ii) energy yield analysis; and (iii) economic analysis. The optimum criteria, including economic and technical feasibility parameters, were analysed using the HOMER software package developed by the U.S. National Renewable Energy Laboratory (NREL).

Moreover, the comparison between the proposed hybrid SPV with WTG power system and the classical solution “diesel generator (DG)” was evaluated in terms of: (i) OPEX savings, where the result showed that the OPEX savings is up to \$27,832 (representing 48.52%); and (ii) GHG emissions, with the CO<sub>2</sub> emissions decreasing to zero.

Finally, many contributions have been provided, such as decreasing OPEX and gas emissions, ensuring sustainability with better cellular network planning and providing cleaner energy, with an emphasis on the application of optimization methods in power system operation and planning.

**Acknowledgments:** This work was supported by the faculty research fund of Sejong University in 2016. We thank the reviewers for the fruitful suggestions, which helped us to improve the quality of this work.

**Author Contributions:** Mohammed H. Alsharif analyzed the data and completed the first draft, and Jeong Kim wrote the solar radiation and wind speed in South Korea and revised the final version of paper.

**Conflicts of Interest:** The authors declare that they have no competing interests.

## Abbreviations

BB	BaseBand
BS	Base Station
CDMA	Code Division Multiple Access
CO <sub>2</sub> , NO <sub>x</sub> , SO <sub>2</sub>	Carbon dioxide, Nitrogen oxides, Sulfur dioxide
CRF	Capital Recovery Factor
DG	Diesel Generator
DOD	Depth of Discharge
FC	Fuel Cell
GHG	GreenHouse Gas
GSM	Global System for Mobile Communication
HOMER	Hybrid Optimisation Model for Electric Renewables
IC	Initial Costs

KMA	Korea Meteorological Administration
LTE	Long Term Evolution
MIMO	Multiple-Input and Multiple-Output
MSW	Modified Sine-Wave
NPC	Net Present Cost
NREL	National Renewable Energy Laboratory
O&M	Operation and Maintenance Costs
OPEX	Operational EXpenditure
PA	Power Amplifier
PSH	Peak Solar Hours
RF	Radio-Frequency
SCR	Solar Control Regulator
SOC	State of Charge
SPV	Solar Photovoltaic
STC	Standard Test Conditions
TAC	Total Annualised Cost
WTG	Wind Turbine Generator

## Symbols

$P_{op}$	BS operating power
$P_{DC}^{PA}$	Power consumed by power amplifier
$P_{DC}^{RF}$	Radio frequency power
$P_{DC}^{BB}$	Baseband power
$P_{tx}^{max}$	BS transmission power
$P_o$	Normalized BS transmission power
$P_{BS}$	Total Power Consumption for the BS
$P_{mc}$	Microwave backhaul power
$P_{lm}$	Auxiliary equipment power
$\sigma_{DC}$	DC-DC power supply losses
$\sigma_{cool}$	Cooling losses
$N_{TRX}$	Number of transceivers
$\eta_{PA}$	PA efficiency
$\alpha$	Path loss coefficient
$R_o$	Coverage radius
$E_{PV}$	Energy output of the PV array
$Y_{PV}$	Rated capacity of the PV array
$f_{PV}$	PV derating factor
$A_{batt}$	Battery bank autonomy
$N_{batt}$	Number of batteries
$V_{nom}$	Nominal voltage of a single battery
$Q_{nom}$	Nominal capacity of a single battery
$L_{prim,ave}$	Average daily LTE-macro BS load
$R_{batt}$	Battery bank lifetime
$Q_{lifetime}$	Lifetime throughput of a single battery
$Q_{thrp}$	Annual battery throughput
$R_{batt,f}$	Battery float life

## References

- 3GPP System Standards. Available online: [http://www.3gpp.org/news-events/3gpp-news/1614-sa\\_5g](http://www.3gpp.org/news-events/3gpp-news/1614-sa_5g) (accessed on 30 July 2016).
- Netmanias Report, LTE in Korea. Available online: <http://www.netmanias.com/en/post/reports/6060/kt-korea-ig-u-lte-lte-a-sk-telecom-wideband-lte/lte-in-korea-2013> (accessed on 30 July 2016).
- Open Signal. Available online: <http://opensignal.com/reports/2016/02/state-of-lte-q4-2015/> (accessed on 30 July 2016).
- Alsharif, M.H.; Nordin, R.; Ismail, M. Survey of Green Radio Communications Networks: Techniques and Recent Advances. *J. Comput. Netw. Commun.* **2013**, *2013*, 453893. [[CrossRef](#)]
- Alsharif, M.H.; Nordin, R.; Ismail, M. Classification, recent advances and research challenges in energy efficient cellular networks. *Wirel. Pers. Commun.* **2014**, *77*, 1249–1269. [[CrossRef](#)]
- Aris, A.M.; Shabani, B. Sustainable power supply solutions for off-grid base stations. *Energies* **2015**, *8*, 10904–10941. [[CrossRef](#)]

7. Kusakana, K.; Vermaak, H.J. Hybrid Renewable Power Systems for Mobile Telephony Base Stations in Developing Countries. *Renew. Energy* **2013**, *51*, 419–425. [[CrossRef](#)]
8. Seoin, B.; Heetae, K.; Hyun, J.C. Optimal Hybrid Renewable Power System for an Emerging Island of South Korea: The Case of Yeongjong Island. *Sustainability* **2015**, *7*, 13985–14001.
9. Ng, D.W.K.; Lo, E.S.; Schober, R. Energy-Efficient Resource Allocation in OFDMA Systems with Hybrid Energy Harvesting Base Station. *IEEE Trans. Wirel. Commun.* **2013**, *12*, 3412–3427. [[CrossRef](#)]
10. Ahmed, I.; Ikhlef, A.; Ng, D.W.K.; Schober, R. Power Allocation for an Energy Harvesting Transmitter with Hybrid Energy Sources. *IEEE Trans. Wirel. Commun.* **2013**, *12*, 6255–6267. [[CrossRef](#)]
11. Martínez-Díaz, M.; Villafáfila-Robles, R.; Montesinos-Miracle, D.; Sudrià-Andreu, A. Study of Optimization Design Criteria for Stand-Alone Hybrid Renewable Power Systems. In Proceedings of the International Conference on Renewable Energies and Power Quality (ICREPQ'13), Bilbao, Spain, 20–22 March 2013; pp. 1–5.
12. Kaldellis, J. Optimum hybrid photovoltaic-based solution for remote telecommunication stations. *Renew. Energy* **2010**, *35*, 2307–2315. [[CrossRef](#)]
13. Serincan, M.F. Reliability considerations of a fuel cell backup power system for telecom applications. *J. Power Sources* **2016**, *309*, 66–75. [[CrossRef](#)]
14. Belkhiri, S.; Chaker, A. Optimization of Hybrid PV/Wind System for Remote Telecom Station, a Case Study of Different Sites in Algeria. In Proceedings of the Chemical, Biological and Environmental Engineering, Ho Chi Minh City, Vietnam, 23–25 March 2016; pp. 1–7.
15. Hossam, K.; Mikhail, A.R.; Hafez, I.M.; Anis, W.R. Optimum Design of PV Systems for BTS in Remote and Urban Areas. *Int. J. Sci. Technol. Res.* **2016**, *5*, 1–9.
16. Salih, T.; Wang, Y.; Adam, M.A.A. Renewable micro hybrid system of solar panel and wind turbine for telecommunication equipment in remote areas in Sudan. *Energy Procedia* **2014**, *61*, 80–83. [[CrossRef](#)]
17. Imtiaz, A.W.; Hafeez, K. Stand Alone PV System for Remote Cell Site in Swat Valley. In Proceedings of the 1st International Conference on Technology and Business Management, Peshawar, Pakistan, 2–4 April 2013; pp. 1–5.
18. Nema, P.; Nema, R.; Rangnekar, S. Minimization of Green House Gases Emission by Using Hybrid Energy System for Telephony Base Station Site Application. *Renew. Sustain. Energy Rev.* **2010**, *14*, 1635–1639. [[CrossRef](#)]
19. Moury, S.; Khandoker, N.M.; Haider, M.S. Feasibility Study of Solar PV Arrays in Grid Connected Cellular BTS Sites. In Proceedings of the 2012 IEEE International Conference on Advances in Power Conversion and Energy Technologies (APCET), Mylavaram, India, 2–4 August 2012; pp. 1–5.
20. Groupe Speciale Mobile Association. *Green Power for Mobile bi Annual Report 2014*; Groupe Speciale Mobile Association (GSMA): London, UK, 2014.
21. Imran, M.; Katranaras, E.; Auer, G.; Blume, O.; Giannini, V.; Godor, I.; Jading, Y.; Olsson, M.; Sabella, D.; Skillermark, P. *Energy Efficiency Analysis of the Reference Systems, Areas of Improvements and Target Breakdown*; Technical Report, ICT-EARTH Deliverable D2.3; EC-IST Office: Brussels, Belgium, 2011.
22. Auer, G.; Giannini, V.; Desset, C.; Godor, I.; Skillermark, P.; Olsson, M.; Imran, M.A.; Sabella, D.; Gonzalez, M.J.; Blume, O. How much energy is needed to run a wireless network? *IEEE Wirel. Commun.* **2011**, *18*, 40–49. [[CrossRef](#)]
23. Schmitt, G. The Green Base Station. In Proceedings of the 4th International Conference on Telecommunication—Energy Special Conference (TELESCON), Frankfurt, Germany, 10–13 May 2009; pp. 1–6.
24. Lambert, T.; Gilman, P.; Lilienthal, P. Micropower System Modeling with HOMER. 2006. Available online: <http://homerenergy.com/documents/MicropowerSystemModelingWithHOMER.pdf> (accessed on 30 July 2016).
25. Alsharif, M.H.; Nordin, R.; Ismail, M. Energy optimisation of hybrid off-grid system for remote telecommunication base station deployment in Malaysia. *EURASIP J. Wirel. Commun. Netw.* **2015**, *2015*, 1–15. [[CrossRef](#)]
26. KMA, Annual Climatological Report 2013, Korea Meteorological Administration. Available online: [http://www.kma.go.kr/weather/observation/data\\_monthly.jsp](http://www.kma.go.kr/weather/observation/data_monthly.jsp) (accessed on 30 July 2016).

27. NASA. Available online: [https://eosweb.larc.nasa.gov/cgi-bin/sse/homer.cgi?email=skip%40larc.nasa.gov&step=1&lat=37.499&lon=126.54958&submit=Submit&ms=1&ds=1&ys=1998&me=12&de=31&ye=1998&daily=swv\\_dwn](https://eosweb.larc.nasa.gov/cgi-bin/sse/homer.cgi?email=skip%40larc.nasa.gov&step=1&lat=37.499&lon=126.54958&submit=Submit&ms=1&ds=1&ys=1998&me=12&de=31&ye=1998&daily=swv_dwn) (accessed on 30 July 2016).
28. Alsharif, M.H.; Kim, J. Optimal Solar Power System for Remote Telecommunication Base Stations: A Case Study Based on the Characteristics of South Korea's Solar Radiation Exposure. *Sustainability* **2016**, *8*, 942. [[CrossRef](#)]
29. NIMS. Available online: [http://www.greenmap.go.kr/02\\_data/data01.do#2#1#1](http://www.greenmap.go.kr/02_data/data01.do#2#1#1) (accessed on 19 August 2016).
30. The Bank of Korea Monetary Policy. Available online: <http://www.bok.or.kr/baserate/baserateList.action?%20menuNaviId=33> (accessed on 30 July 2016).
31. Ge, X.; Cheng, H.; Guizani, M.; Han, T. 5G wireless backhaul networks: Challenges and research advances. *IEEE Netw.* **2014**, *28*, 6–11. [[CrossRef](#)]
32. Sharp Solar Electricity Incorporation. Available online: <http://www.sharp-world.com/solar/en/solutions/index.html> (accessed on 30 July 2016).
33. FT-1000L Wind Turbine Generator Model. Available online: [http://www.chinaseniorsupplier.com/Electrical\\_Equipment\\_Supplies/Generators/60423002878/Home\\_use\\_1000w\\_wind\\_turbine\\_generator\\_manufacturer.html](http://www.chinaseniorsupplier.com/Electrical_Equipment_Supplies/Generators/60423002878/Home_use_1000w_wind_turbine_generator_manufacturer.html) (accessed on 30 July 2016).
34. Trojan Battery Incorporation. Available online: <http://www.trojanbattery.com/> (accessed on 30 July 2016).
35. Leonics Incorporation, SolarCon SPT-Series. Available online: [http://www.leonics.com/product/renewable/solar\\_charge\\_controller/dl/spt-074.pdf](http://www.leonics.com/product/renewable/solar_charge_controller/dl/spt-074.pdf) (accessed on 30 July 2016).
36. Global Petrol Prices. Available online: [http://www.globalpetrolprices.com/South-Korea/diesel\\_prices/](http://www.globalpetrolprices.com/South-Korea/diesel_prices/) (accessed on 30 July 2016).
37. Calculation of CO<sub>2</sub> Emissions. Available online: [http://people.exeter.ac.uk/TWDavies/energy\\_conversion/Calculation%20of%20CO2%20emissions%20from%20fuels.htm](http://people.exeter.ac.uk/TWDavies/energy_conversion/Calculation%20of%20CO2%20emissions%20from%20fuels.htm) (accessed on 30 July 2016).



© 2016 by the authors; licensee MDPI, Basel, Switzerland. This article is an open access article distributed under the terms and conditions of the Creative Commons Attribution (CC-BY) license (<http://creativecommons.org/licenses/by/4.0/>).